# Nanocomposite Materials of Thermoplastic Polymers Reinforced by Polysaccharide

**ARTICLE** *in* ACS SYMPOSIUM SERIES · MARCH 1999

DOI: 10.1021/bk-1999-0723.ch003



**3 AUTHORS**, INCLUDING:

Alain Dufresne
Grenoble Institute of Technology
**312** PUBLICATIONS **15,264** CITATIONS
SEE PROFILE

J.-Y. Cavaillé
Institut National des Sciences Appliquées de Lyon
**272** PUBLICATIONS **6,267** CITATIONS
SEE PROFILE

99.13

Chapter 3

# Nanocomposite Materials of Thermoplastic Polymers Reinforced by Polysaccharide

**A. Dufresne and J. Y. Cavaillé[1]**

**Centre de Recherches sur les Macromolécules Végétales (CERMAV-CNRS), Université Joseph Fourier, BP 53, 38041 Grenoble Cedex 9, France**

Biosynthesis of starch leads to semicrystalline systems, in which highly crystalline domains are embedded in an amorphous matrix. The average size of such microcrystals is a few tens of nm. In the case of cellulose, microfibrils are biosynthesized and deposited in a continuous fashion. This mode of biogenesis can lead to crystalline microfibrils with a high aspect ratio, almost defect free, and axial mechanical properties approaching those of perfect crystals. The use of such microcrystals, as reinforcing fillers in thermoplastic matrices leads to nanocomposite materials. In this work, we will focus on different materials, and we will see that in addition to some practical applications, their study can help to understand some physical properties as geometric and mechanical percolation effects.

Natural polysaccharide fillers are gaining attention as a reinforcing phase in thermoplastic matrices (*1-3*). Low density, highly reduced wear of processing machinery and a relatively reactive surface may be mentioned as attractive properties, together with abundance and low price. Moreover, the recycling by combustion of polysaccharide filled composites is easier in comparison with inorganic filled systems. Nevertheless, such fillers are used only to a limited extent in industrial practice, which may be explained by difficulties in achieving acceptable dispersion levels.

An alternative way to palliate this restriction consists of using a latex to form the matrix. Indeed, it is well known that emulsion polymerization can lead to materials easily processed, either by film casting techniques (water evaporation for paint applications for example) or by freeze drying (or more simply by flocculation) followed by a classical extrusion process. As a matter of fact, different monomers can be statistically copolymerized to adjust the glass-rubber transition temperature (*4*).

[1]Current address: GEMPPM, UMR CNRS-INSA #55, INSA Lyon, F-69621 Villeurbanne Cedex, France.

More generally, it is also possible to mix different types of water suspensions, including some polymer latices and organic or inorganic stabilized suspensions. In this work, various polysaccharide fillers are used and the behavior of the resulting nanocomposite materials is analyzed as a function of the aspect ratio (L/d, L being the length and d the aspect ratio).

## Experimental

**Transmission Electron Microscopy.** All observations were made with a Philips CM200 electron microscope. A drop of a dilute suspension of microcrystalline polysaccharide filler was deposited and allowed to dry on a carbon coated grid.

**Starch Microcrystals.** Starch microcrystals, which are mainly formed of amylose, were prepared by acid hydrolysis of the amorphous domains of potato starch granules obtained from Sigma (Ref. 9005-25-8) as previously reported (*5*). They occur as a finely divided white powder, insoluble in water. Starch granules were first hydrolyzed with hydrochloric acid. This suspension (5% w/w of solid component in water) was stored at 35°C for 15 days. This period of time allows removal of the amorphous zones without damaging the crystalline zones. The suspension was stirred every day in order to ensure the homogeneity of the suspension. It was then diluted with an equal volume of distilled water and washed by successive centrifugation (4,000 trs/min) until acid free. The dispersion of microcrystals was completed by a further 3 min ultrasonic treatment (B12 Branson sonifier). The solid fraction of this aqueous suspension was determined to be around 1.5%. A typical electron micrograph obtained from the dilute suspension of hydrolyzed starch is shown in Figure 1a. It consists of starch fragments which have a homogeneous distribution in size. Each fragment contains associated microcrystals which are not clearly identified. The microcrystals are a few tens of nm in diameter and their aspect ratio is around 1.

**Cellulose Microcrystals.** Two sources of cellulose whiskers were used. One source was whiskers from tunicin, an animal cellulose whose microfibrils are particularly well organized and crystallized. The second source was from wheat straw cellulose.

**Cellulose Whiskers from Tunicin.** Suspensions of tunicin whiskers in water were prepared as described elsewhere (*6,7*). A batch of edible-grade tunicate (*Microcosmus fulcatus*), from the Mediterranean, was obtained from a local fish shop. After anesthetizing with chloroform, the animals were gutted and their tunic was cut into small fragments that were deproteinized by three successive bleaching treatments, following the method of Wise *et al.* (*8*). The bleached mantles (the "tunicin") were then disintegrated in water with a Waring blender (at a concentration of 5% by weight). The resulting aqueous tunicin suspension was mixed with $H_2SO_4$ to reach a final acid/water concentration of 55% (weight fraction). Hydrolysis conditions were 60°C for 20 min under strong stirring. A dispersion of cellulose whiskers resulted. After sonication, the

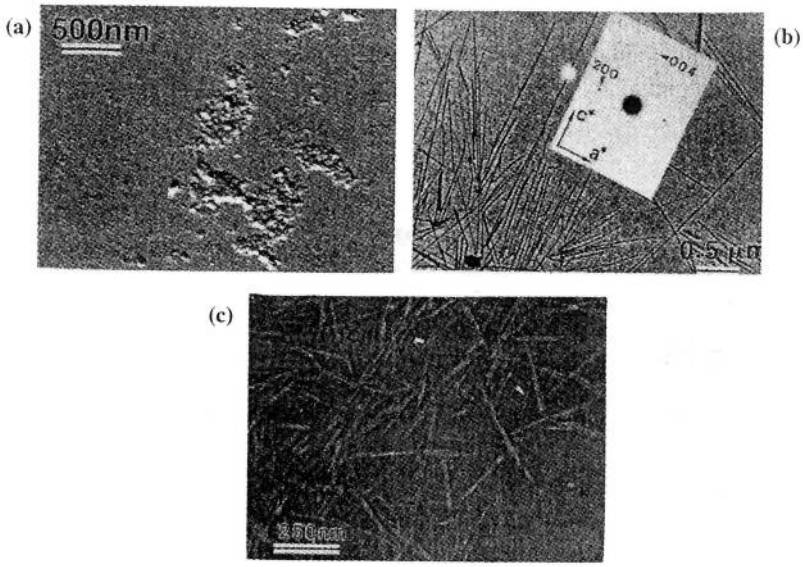


Figure 1. Transmission electron micrographs from a dilute suspension of : (a) hydrolyzed potato starch (Reproduced with permission from ref. 5. Copyright 1996 American Chemical Society), (b) hydrolyzed tunicin (inset: typical electron diffractogram recorded on one microcrystal), and (c) hydrolyzed wheat straw cellulose.

suspension was neutralized and washed by dialysis. It did not sediment or flocculate as a consequence of surface sulfate groups created during the sulfuric acid treatment (*9*). When concentrated by evaporation, the suspensions displayed typical liquid crystal characteristics (*9,10*).

A typical preparation of tunicin crystals is shown in Figure 1b. This sample consists of parallel rods with lengths ranging from 100 nm to several micrometers and widths on the order of 10-20 nm. The aspect ratio of these whiskers is, therefore, around 100. Upon testing by a microelectron diffraction technique (inset), each element gave a spot diffractogram that corresponded to a section of the reciprocal lattice of cellulose Iβ (here the a*c* section) and persisted when the electron probe was scanned along a given rod. The diffractogram indicated that the cellulose chain axis is along the long dimension of the rods. Each rod is, therefore, a whisker-like tunicin crystal with no apparent defect.

**Cellulose Whiskers from Wheat Straw.** The starting raw material used to prepare microcrystalline wheat straw cellulose was steam exploded wheat straw. The wheat straw was first hydrolyzed in an aqueous solution of sodium sulfite (5% v/v). Material was placed in a steam explosion reactor, developed at CERMAV (*11*), for 4 min at 210°C under a vapor pressure of 19.5 bars. The pressure was then rapidly released. Next, the material was washed with cold water to remove solubles. The steam exploded straw cellulose (20 wt% solids in water) was washed 6 times in boiling 2% sodium hydroxide for 4 hours under mechanical stirring. Cellulose was then bleached with a chlorite solution to a high brightness level.

Stable colloidal dispersions of straw cellulose were prepared according to a previously described method (*12*). The aqueous suspension of cellulose (5 wt% of filtered cellulose) was first hydrolyzed with sulfuric acid. The microcrystalline suspension was then dialyzed against distilled water until neutrality was obtained. The dispersion of cellulose microcrystals was completed by a 3 min ultrasonic treatment (B12 Branson sonifier).

A typical electron micrograph obtained from a dilute suspension of hydrolyzed straw cellulose is shown in Figure 1c. The dried suspension was negatively stained with uranyl acetate. This treatment reveals individual microcrystals (indicated by arrows) and associated microcrystals. Individual microcrystals are rods of 150 to 300 nm in length with widths close to 5 nm. This latter value corresponds to a close packing of about 40 chains of cellulose. The aspect ratio of these whiskers is, therefore, around 45.

**Polysaccharide Filler/Latex Composites.** In order to process nanocomposite materials with a good level of dispersion, the thermoplastic matrix used was an aqueous suspension of polymer, i.e. a latex. The latex used for the matrix was obtained by copolymerization of styrene (34 wt%) with butyl acrylate (64 wt%) and was provided by Elf-Atochem (Serquigny, France). It contains 1% acrylic acid and 1% acrylamide. It will be referred to as poly(S-co-BuA). The aqueous suspension contained spherical

particles with an average diameter around 150 nm and had a 50 wt% solid fraction. The glass-rubber transition temperature (Tg) of the copolymer was around 0°C.

Various amounts of the colloidal microcrystalline starch dispersion or cellulose whisker suspension were mixed with the suspension of latex to adjust film composition. After stirring, the preparations were cast and evaporated (samples labeled E). In order to test the effect of the processing technique on the mechanical behavior of the nanocomposite materials, films were also processed by freeze-drying and molding the preparations using wheat straw cellulose whiskers as filler (samples labeled P). Hot-pressing was performed with a Carver Laboratory Press at 140 bar for 30 min at 90°C.

**Dynamic Mechanical Analysis.** Dynamic mechanical tests were carried out in the glass-rubber transition temperature range of poly(S-co-BuA) with two kinds of apparatus. The first one was an RSA2 spectrometer from Rheometrics, working in the tensile mode. This setup measured the complex tensile modulus E*; i.e., the storage component E' and the loss component E". Measurements were performed under isochronal conditions at 1 Hz and temperature was varied by steps of 3 K. The second apparatus used was a mechanical spectrometer (Mecanalyseur) from METRAVIB SA (Ecully, France). The device consists of a forced oscillation pendulum. It provides the real (G') and imaginary (G") parts of the shear modulus and the internal friction coefficient ($\tan \phi = G''/G'$) as a function of frequency and/or temperature. Temperature scans were performed in the range 200 to 500 K at a fixed frequency (0.1 Hz).

**Water Uptake.** Polysaccharides are hygroscopic material and water diffusion behavior will depend on composition. The use of hydrophilic fillers as a dispersed phase in a hydrophobic matrix protects against moisture. However, if the adhesion level between the filler and the matrix is not good, diffusion pathways can exist or can be created by mechanical solicitation. The existence of such pathways is also related to filler connection and, therefore, to its percolation threshold. The kinetics of absorption were determined for all the microcrystalline starch/poly(S-co-BuA) compositions. The specimens used to analyze the water absorption were thin rectangular strips with dimensions of 10 mm × 10 mm × 1 mm. The films were considered to be thin enough such that molecular diffusion was one-dimensional.

Samples were first dried for one night at 70°C. After cooling to room temperature and weighing the samples, they were immersed in distilled water. The water temperature was maintained at 25±0.5°C. Samples were then periodically removed from the water, gently blotted with tissue paper to remove the excess water on the surface, and immediately weighed on a four-digit analytical balance. In order to evaluate the water uptake of the starch microcrystal filled composite materials, the increase in weight was measured after various times of exposure to water. The weight percentage increase was calculated as follows :

$$\text{water uptake (\%)} = \frac{M_t - M_o}{M_o} \times 100 \qquad (1)$$

where $M_t$ and $M_o$ are the weights after t min exposure to water and before exposure to water, respectively. The mass of water absorbed at time t, ($M_t$-$M_o$), can be expressed at short times (corresponding to $(M_t-M_o)/M_\infty \leq 0.5$) as reported by Comyn (*13*):

$$\frac{M_t - M_o}{M_\infty} = \frac{2}{L}\left(\frac{D}{\pi}\right)^{1/2} t^{1/2} \qquad (2)$$

where $M_\infty$ is the mass absorbed at equilibrium, 2L is the thickness of the film and D is the diffusion coefficient.

## Results and Discussion

**Starch Microcrystal Based Nanocomposites.** The mechanical behavior and the water uptake of the starch microcrystal/poly(S-co-BuA) films were analyzed as a function of the material composition (pure matrix to 60 wt% starch microcrystal filled composites).

**Mechanical Behavior.** Dynamic mechanical tests were performed in the glass-rubber transition range of the matrix (*5*, Dufresne, A.; Cavaillé, J.Y. *J. Polym. Sci., Part B*, in press). The plot of log(E'/Pa) (storage tensile modulus) versus temperature at 1 Hz is displayed in Figure 2. The curve corresponding to the pure matrix (0% filled composite) is typical of thermoplastic behavior. For temperatures below the Tg, the copolymer is in the glassy state. The modulus decreases slightly with temperature, but remains roughly constant (around 2 GPa). Then, a rapid decrease in the elastic tensile modulus, more than three (3) orders of magnitude, is observed, corresponding to the glass-rubber transition. In the terminal zone, the elastic tensile modulus becomes lower with temperature and can not be experimentally measured.

At the utilized filler concentrations, there are on the order of 200,000 to 400,000 $cm^2$ of filler surfaces/$cm^3$ of material. Therefore, neglecting the likely agglomeration of the filler, the average interparticle distance is on the order of the filler diameter. This should have an effect on conformational properties and will certainly result in significant increases in the Tg of the matrix. However, the observation that should be emphasized is that the temperature of the modulus drop associated with the Tg remains almost constant, whatever the concentration of filler (*5*).

For temperatures below the Tg, the composite modulus increases up to 4 GPa for the 60% filled material. However, the exact determination of the glassy modulus depends on the precise knowledge of the sample dimensions. In this case, at room temperature, the composite films were soft and it was difficult to determine precisely sample thickness. In order to minimize this, the samples were frozen in liquid nitrogen prior to experimentation to accurately measure their dimensions.

Above the Tg, a greater increase in the composite modulus is observed with increasing volumes of microcrystalline starch. For instance, the relaxed modulus at the Tg + 50°C (~ 325 K) of a film containing only 30% starch is 100-fold higher than that

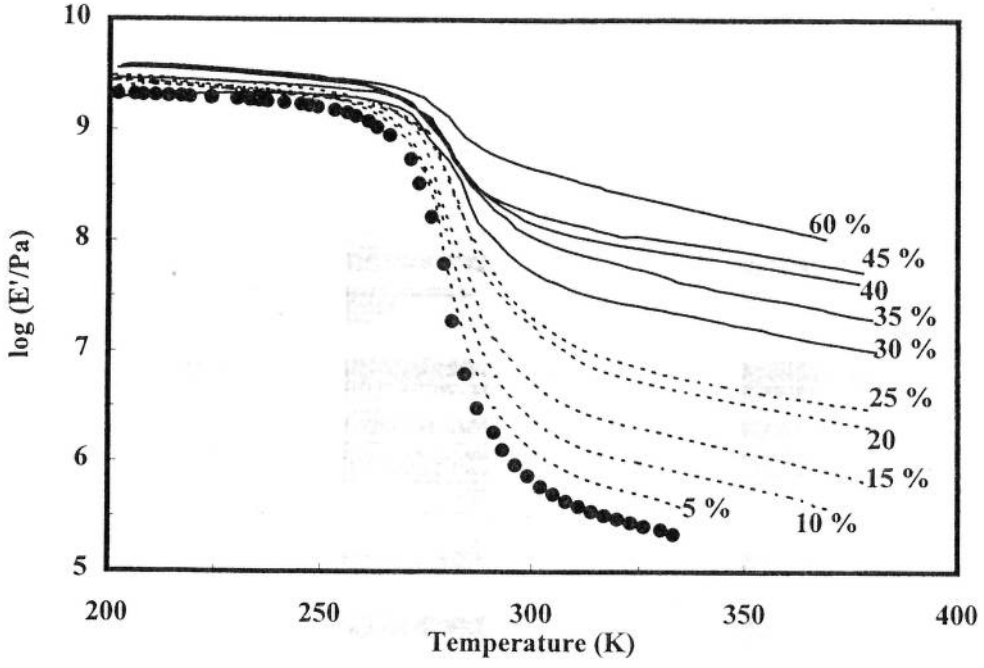


Figure 2. Storage tensile modulus E' versus temperature at 1 Hz for composites reinforced by weight fractions of starch microcrystals from 0 to 60 wt%: (●) 0%, (---) low filler content, and (—) high filler content.

of the matrix. For the 60% microcrystalline cellulose filled composite, the relaxed modulus is increased about 1000-fold. The experimental data show two sets of relaxed moduli, depending on the material composition. The first one (see dashed lines in Figure 2) corresponds to low starch content composites (from 5 to 25 wt%), and the second one (see continuous line in Figure 2) to highly filled material (from 30 up to 60 wt%). This critical value of 30 wt% more or less corresponds to a filler volume fraction of 20%, which in turn, corresponds to the percolation threshold of isoradius spherical particle filled systems. Therefore, a connection of starch particles or a geometric percolation effect occurs as the filler content approaches 20 vol%.

Starch microcrystals bring a great reinforcing effect, especially at temperatures higher than the Tg of the synthetic matrix (*5*). They can, therefore, be used as an economic and environmentally friendly particulate filler, and can be useful for the processing of stiff small-sized wares. Classical models for polymers comprising nearly spherical particles, based on a mean field approach as generalized by the Kerner equation according to Lewis (*14*) and Nielsen (*15*), were used to predict this behavior (*5*). The Kerner equation and its modifications were derived for spherical particles in a linear elastic matrix. However, this does not imply that it may be applied only below the Tg. Indeed, it is well known that the behavior of polymers is not purely elastic, but rather viscoelastic. For this reason, it is appropriate to modify the relationships for elasticity by introducing viscoelastic moduli; i.e., their complex form $E^*(i\omega,T)$. However, at the temperature at which calculations were performed (325 K), this is not necessary because the storage modulus E' is about 10 times higher than the loss modulus E". Therefore, the error made in taking E as E' is around 10%. It was observed that the calculated moduli from this model do not fit the experimental moduli of the real systems (*5*). This discrepancy is due to the morphology of these nanocomposite systems, and was discussed in light of aggregate formation and percolation concepts (Dufresne, A.; Cavaillé, J.Y. *J. Polym. Sci., Part B*, in press).

**Water Uptake.** The maximum swelling rate, or maximum relative water uptake, of starch microcrystal filled poly(S-co-BuA) was analyzed versus starch content (Dufresne, A.; Cavaillé, J.Y. *J. Polym. Sci., Part B*, in press). Water sensitivity increases linearly with the starch content. This can be easily understood because water uptake reflects an equilibrium state. If the diffusion coefficient of water, D, as calculated from equation 2, is reported as a function of the material composition, two well separated zones are displayed (see Figure 3). Above the percolation threshold (~ 20 vol%), the percolation of starch microcrystals leads to a more abrupt evolution of D versus starch content. The full line corresponds to the prediction of this behavior by a three branch series-parallel model, including the percolation concept which was developed elsewhere (Dufresne, A.; Cavaillé, J.Y. *J. Polym. Sci., Part B*, in press). The discrepancy observed between experimental data and the predicted curve in the high starch content range probably originates from the fact that the value of D used for starch in the model is that observed for native starch, which is certainly higher than that of microcrystalline starch.

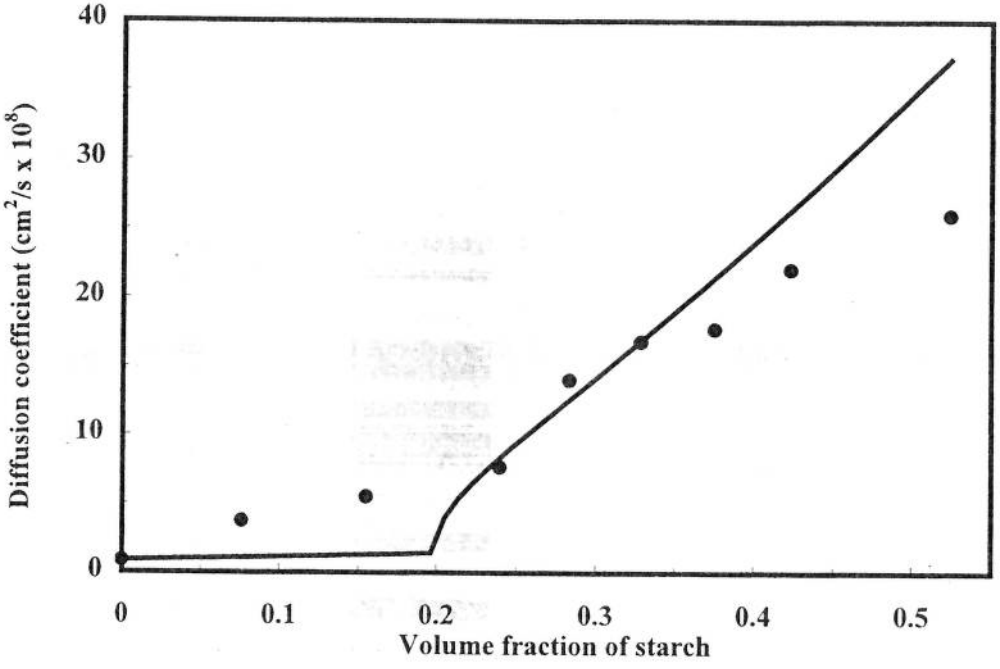


Figure 3. Variation of the diffusion coefficient versus starch content: (●) experimental data, and (—) predicted data from the series-parallel model including the percolation concept.

**Cellulose Whisker Based Nanocomposites.** The mechanical behavior of the cellulose whisker/poly(S-co-BuA) films as analyzed as a function of the material composition utilizing two sources of cellulose whiskers.

**Cellulose Whiskers from Tunicin.** Figure 4 shows the plot of log(G'/Pa) versus temperature for various tunicin whisker compositions ranging from 0 to 14 wt%. When reinforced by a small percentage of whiskers, the polymer films show improved mechanical properties which are particularly striking when the films were heated above the glass transition of the polymer. For temperatures below the Tg, the difference between the elastic shear modulus of the cellulose whiskers (50 GPa) and that of the matrix (1 GPa), is not high enough for an appreciable reinforcement effect. However, this effect exists and is well predicted by models based on a mean-field approach.

Above the Tg, a greater increase in the composite modulus is observed with increasing volume of cellulose, and, therefore, the drop in G value is dramatically reduced. For instance, the relaxed modulus of a film containing only 6 wt% of whiskers is 1000-fold higher than that of the matrix. Moreover, the reinforced films behave like rubber as their modulus value stayed constant over a wide temperature range. This is illustrated in Figure 4. The relaxed modulus of a 6 wt% filled nanocomposite remained near 0.1 GPa up to 500 K, a temperature at which cellulose starts to decompose.

The variation of the relaxed shear modulus G, taken at 325 K (i.e., 50 K above the Tg of the matrix), is plotted as a function of the whisker content in Figure 5. The experimental data (full circles) are much higher than those predicted by a classical mean-field mechanical model developed for short fiber composites (dashed line). In such an approach, following Halpin and Kardos (*16*), the modulus and the geometry of the fibers are accounted for, but one assumes that there is no interaction between the fibers. In particular, the mean-field approach is based on the concept that a material made of short fibers, homogeneously dispersed in a continuous matrix, is mechanically equivalent to a superposition of four plies. Within each ply, the fibers are parallel to one another and the mutual orientation of the plies is 0, +45, +90 and -45°. The mechanical properties of each ply are derived from the micromechanic equations of Halpin-Tsai (*17*).

In order to explain the unusually high G values of the reinforced films, one needs to invoke (i) a strong interaction between the whiskers and (ii) a percolation effect. The influence of such effects on the mechanical properties of the films can be calculated following the method of Ouali *et al.* (*18*) in their adaptation of the percolation concept to the classical parallel-series model of Takayanagi *et al.* (*19*). The shear modulus of the composite is then given by:

$$G = \frac{(1-2\psi+\psi v_R)G_S G_R + (1-v_R)\psi G_R^2}{(1-v_R)G_R + (v_R-\psi)G_S} \qquad (3)$$

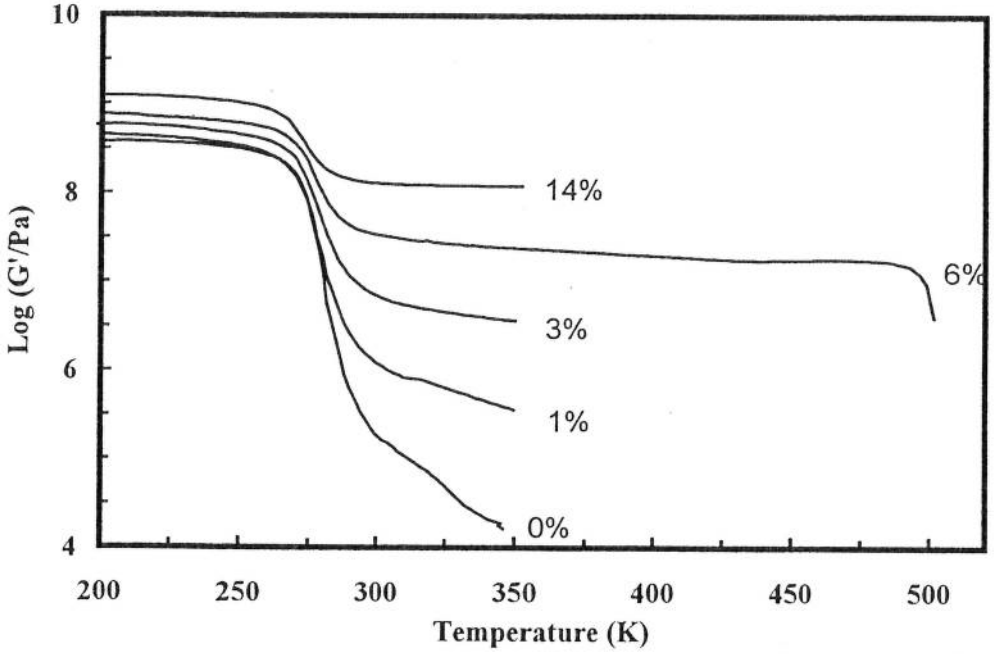


Figure 4. Storage shear modulus G' versus temperature at 0.1 Hz for composites reinforced by weight fractions of tunicin whiskers from 0 to 14%.

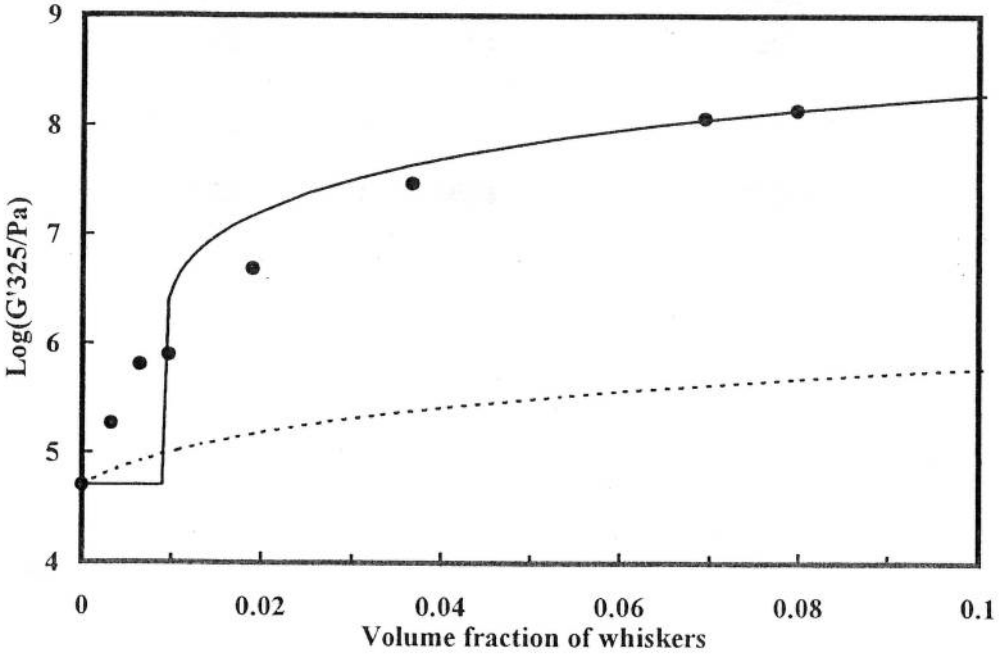


Figure 5. Plot of the logarithm of the storage shear modulus at 325 K as a function of the volume fraction of tunicin whiskers. Comparison between the experimental data (●) and calculated data with two different mechanical models: a mean-field model (dashed line) and a percolation model (continuous line).

where the subscripts S and R refer to the soft and rigid phases, respectively, and $v_R$ is the volume fraction of whiskers. In the Takayanagi *et al.* model (*19*), $\psi$ is an adjustable parameter, whereas in the Ouali *et al.* prediction (*18*), which was used here, $\psi$ corresponds to the volume fraction of the percolating rigid phase. It can be calculated with a simple prediction based on the percolation concept (*18*):

$$\begin{aligned} \psi &= 0 && \text{for } v_R < v_{Rc} \\ \psi &= v_R\left(\frac{v_R - v_{Rc}}{1 - v_{Rc}}\right)^b && \text{for } v_R \geq v_{Rc} \end{aligned} \tag{4}$$

where b is the percolation exponent and $v_{Rc}$ is the percolation threshold, which is close to 1 vol% (i.e. 1.5 wt%) as determined by numerical calculation for sticks with an aspect ratio equal to 100 (*6*). According to several studies based on the percolation concepts (*20,21*), b takes the value of 0.4 in a three-dimensional system.

The calculated curve based on the percolation theory is reported as a solid line in Figure 5. It follows the dashed line up to a whiskers volume fraction of 1%. The discrepancy observed between the calculated curve based on the percolation approach and the experimental data at low filler content is probably due to the fact that the prediction does not account for the length distribution of the whiskers. Above this critical percentage, the solid line precisely fits the experimental G values without adjustable parameters. The role of percolation of cellulose fibers in paper making is well documented (*22,23*). It is, in particular, established that the high mechanical properties of a paper sheet result from the hydrogen-bonding forces that hold the percolating network of the fibers. This hydrogen-bonded system is responsible for the unusual mechanical properties of the cellulose whisker based composites when the percolation threshold is reached. Moreover, this whisker network is also responsible for the stabilization of G over a large temperature range above the Tg. It will be only when the whiskers start to decompose at around 500 K that this stabilization will disappear, inducing a catastrophic decrease of the mechanical behavior. Therefore, although mainly phenomenological, the model based on percolation concepts is able to take into account the microstructural parameters of the composites. Finite element simulations have reinforced the hypothesis that the geometrical percolation of the whiskers has been accounted for in these systems, but they also proved the important role of joints between percolating whiskers. In that regard, stiff links, due to many hydrogen bonds, are thought to exist between connected whiskers, making the whole network very rigid (*24*).

**Cellulose Whiskers from Wheat Straw.** The mechanical behavior of wheat straw cellulose whisker/poly(S-co-BuA) films was analyzed with a spectrometer (RSA2) from Rheometrics working in the tensile mode. When nanocomposite structures were obtained by freeze-drying and molding the mixture of cellulose and

latex (samples P), the mechanical properties are substantially improved by increasing the amount of filler (*12*). Whiskers bring a great reinforcing effect at temperatures higher than the glass transition temperature of the matrix and improve the thermal stability of the composite. However, due to the lower axial aspect ratio of these whiskers in comparison with the tunicin whiskers, the reinforcement is lower. For instance, the relaxed modulus is more than a thousand times higher than that of the matrix for a film containing 30 wt% wheat straw whiskers. Figure 6 displays the relaxed modulus appraised at 325 K (~ Tg + 50K). Experimental data for the freeze-dried and hot pressed samples correspond to the full circles.

Classical models for short fiber composites based on a mean-field approach (Halpin-Kardos model) do not explain this reinforcing effect. It was observed that calculations overestimate the glassy modulus, whereas the rubbery modulus was underestimated. To fit the experimental data over the whole temperature range, interactions between the microcrystals, their topological arrangement, and the probable formation of whisker clusters within the thermoplastic matrix have to be taken into account (*12*). We have fitted the experimental moduli via a Halpin-Kardos-like equation to obtain the best interpolated curve for the entire composition and temperature ranges. From trial and error, it appears that the aspect ratio should be 450 to fit the experimental data (see dashed line in Figure 6). This means that wheat straw cellulose whiskers act as fibers (~ 10 times larger than the real ones), due to strong interactions between whiskers.

The evolution of the experimental relaxed moduli versus composition for the cast and evaporated composite films (samples E) are reported as open circles in Figure 6. It is clear from this plot that this processing technique leads to better mechanical properties than those of materials prepared by freeze-drying and hot-pressing the same mixture. This phenomenon can ensue from two origins:

(i) a strong interaction between the whiskers leading to the formation of a whisker network within the thermoplastic matrix,

(ii) a heterogeneity within the thickness of the composite due to the processing itself, via the evaporation step leading to the sedimentation of the cellulose whiskers, which facilitates network formation (point i).

In order to verify the second, scanning electron microscopy (SEM) was used to characterize the morphology of whisker filled nanocomposite films E (*25*). It was shown that the top face of the sample is lower in cellulose content than the bottom face. This gradient of whisker concentration is probably induced by the processing technique since it is not present in freeze-dried and hot-pressed materials. When the filler content increases, the concentration difference in the sample thickness is not so obvious. To validate this sedimentation phenomenon, wide angle X-ray scattering (WAXS) was used (*25*). Due to the high crystallinity level of the cellulose whiskers and the amorphous state of the polymeric matrix used, it is possible to determine the sedimentation of the filler by simply comparing the diffracted X-ray beam from the two faces of the sample. Differences are in good agreement with filler sedimentation.

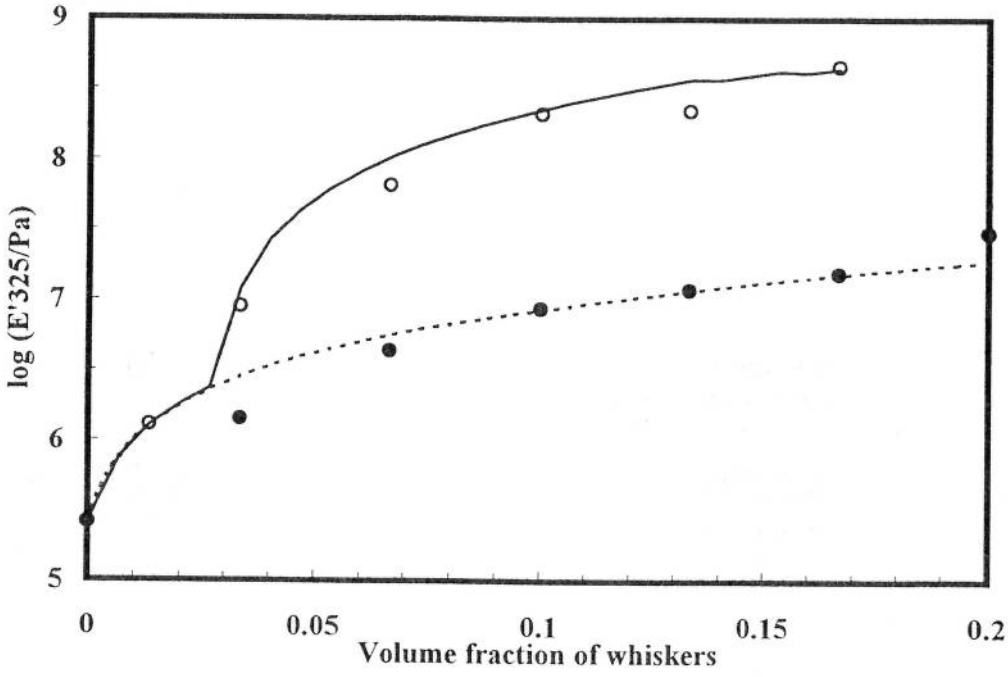


Figure 6. Plot of the logarithm of the storage shear modulus at 325 K as a function of the volume fraction of wheat straw cellulose whiskers. Comparison between the experimental data of freeze-dried and hot pressed (●) and cast and evaporated samples (○), and calculated data with two different mechanical models: a mean-field model (dashed line, L/d = 450) and a multilayered model (continuous line).

The behavior of these composite materials are well described by using a multilayered model consisting of layers parallel to the film surface and described by Dufresne *et al.* (*25*). Assuming a concentration gradient in the film thickness, the modulus of the specimen was calculated from the modulus of each layer. The modulus of each layer was predicted from a model based either on a mean field approach (Halpin-Kardos model), or on a percolation approach dependent on the volume fraction of whiskers in a given layer with respect to the critical volume fraction at the percolation threshold. The very large reinforcing effect reported for the cast and evaporated materials is, therefore, attributed on one hand to the sedimentation of the filler during the evaporation step and on the other hand to the formation of a rigid network, probably linked by hydrogen bonds. The formation of this network is assumed to be governed by a percolation mechanism. The predicted curve from this multilayered model is reported in Figure 6 (see full line), whereas open circles refer to the experimental data.

## Conclusions

The present contribution, reporting work performed on the processing and behavior of new nanocomposite materials of thermoplastic polymers reinforced by polysaccharide microcrystals, is an effort aimed at providing further knowledge to a research area facing a variety of pending issues. It was shown that the reinforcing effect of a particulate filler (starch microcrystals with an aspect ratio of 1) is only due to the geometrical percolation of the filler. Increasing the aspect ratio of the filler (~ 100 for tunicin whiskers), leads to a mechanical percolation phenomenon and enhanced mechanical properties through the formation of a rigid filler network. The lower axial aspect ratio of wheat straw whiskers in comparison to the tunicin whiskers induces two main differences, namely (i) a poorer dispersion level of the filler within the synthetic polymeric matrix and (ii) a sedimentation phenomenon occurring during the evaporation step. For this latter system, mean-field effects and mechanical percolation effects coexist and the predominance of one over the other is a function of the composition of the considered layer.

The processing of fully biodegradable composites based on poly (hydroxyoctanoate) (PHO) and using starch microcrystals or cellulose whiskers as fillers, was also investigated. The results will be published shortly. The first step of this work was to purify the polymer from biomass and obtain a stable latex without degradation of the polymer (*25*). Cellulose can also be used as a microfibrillar filler, which is attractive in terms of available amounts and preparation. The mechanical behavior is then very sensitive to the degree of cellulose purification and the individual state of cellulose microfibrils (*26*). Nanocomposite materials were also prepared and characterized using potato cellulose microfibrils as the filler and potato starch as the matrix (Dufresne, A.; Vignon, M.R. *Macromolecules*, in press.).

**Acknowledgments**

Authors gratefully acknowledge coworkers who participated in results presented in this paper: Dr. H. Chanzy, Dr. V. Favier, and Dr. W. Helbert.

**Literature Cited**

1. Klason, C.; Kubat, J.; Strömvall, H.E. *Int. J. Polym. Mater.* **1984**, *10*, 159.
2. Zadorecki, P.; Michell, A. J. *Polym. Compos.* **1989**, *10*, 69.
3. Maldas, D.; Kokta, B. B.; Daneault, C. *Int. J. Polym. Mater.* **1989**, *12*, 297.
4. Schlund, B.; Guillot, J.; Pichot, C. *Polymer* **1989**, *60*, 1883.
5. Dufresne, A.; Cavaillé, J. Y.; Helbert, W. *Macromolecules* **1996**, *29*, 7624.
6. Favier, V.; Canova, G.R.; Cavaillé, J.Y.; Chanzy, H.; Dufresne, A.; Gauthier, C. *Polym. Adv. Tech.* **1995**, *6*, 351.
7. Favier, V.; Chanzy, H.; Cavaillé, J. Y. *Macromolecules* **1995**, *28*, 6365.
8. Wise, L. E.; Murphy, M.; D'Addiecco, A. A. *Pap Trade J.* **1946**, *122*, 35.
9. Marchessault, R. H.; Morehead, F. F.; Walter, N. M. *Nature* **1959**, *184*, 632.
10. Revol, J. F.; Bradford, H., Giasson, J.; Marchessault, R. H.; Gray, D. G. *Int. J. Biol. Macromol.* **1992**, *14*, 170.
11. Excoffier, G.; Toussaint, B.; Vignon, M. R. *Biotechnol. Bioeng.* **1991**, *38*, 1308.
12. Helbert, W; Cavaillé, J. Y., Dufresne, A. *Polym. Compos.* **1996**, *17*, 4, 604.
13. Comyn, J. *Polymer Permeability*; Comyn, J., Ed.; Elsevier Applied Science: New York, NY, **1985**.
14. Lewis, T. B.; Nielsen, L. E. *J. Appl. Mater. Sci.* **1970**, *14*, 1449.
15. Nielsen, L. E. *J. Appl. Phys.* **1970**, *41*, 4626.
16. Halpin, J. C.; Kardos, J. L. *J. Appl. Phys.* **1972**, *43*, 2235.
17. Tsai, S. W., Halpin, J. C.; Pagano, N. J. *Composite Materials Workshop;* Technomic: Stanford, CT, **1969**.
18. Ouali, N.; Cavaillé, J. Y.; Pérez, J. *J. Plast., Rubber Comp. Process. Appl.* **1991**, *16*, 55.
19. Takayanagi, M.; Uemura, S.; Minami, S. *J. Polym. Sci., Part C* **1964**, *5*, 113.
20. Stauffer, D. *Introduction to Percolation Theory*; Taylor and Francis: London and Philadelphia, **1985**.
21. de Gennes, P.-G. *Scaling Concepts in Polymer Physics*; Cornell University Press: Ithaca, NY, **1979**.
22. Batten, G. L. Jr.; Nissan, A. H. *TAPPI* **1987**, *70*, 119.
23. Nissan, A. H.; Batten, G. L. Jr. *TAPPI* **1987**, *70*, 128.
24. Favier, V.; Dendievel, R.; Canova, G. R.; Cavaillé, J. Y. *Acta Mater.* **1997**, *45*, 1557.
25. Dufresne, A.; Cavaillé, J. Y.; Helbert, W. *Polym. Compos.* **1997**, *18*, 2, 198.
26. Dufresne, A.; Cavaillé, J. Y.; Vignon, M. R. *J. Appl. Polym. Sci.* **1997**, *6*, 1185.